Korean J. Chem. Eng., 39(12), 3452-3463 (2022)
DOI: 10.1007/s11814-022-1217-x

pISSN: 0256-1115
eISSN: 1975-7220

Predictions of thermodynamic properties of pure fluids, refrigerants, and binary mixtures using modified Peng-Robinson equation of state

Pradnya Nirmala Prabhakar Ghoderao*, Mohan Narayan, Vishwanath Haily Dalvi***, and Hun-Soo Byun*,†**

*Department of Chemical and Biomolecular Engineering, Chonnam National University, Yeosu, Jeonnam 59626, Korea
**Department of Physics, Institute of Chemical Technology, Mumbai-400019, India
***Department of Chemical Engineering, Institute of Chemical Technology, Mumbai-400019, India
(*Received 29 April 2022 • Revised 24 June 2022 • Accepted 29 June 2022*)

Abstract−The Peng-Robinson (PR) EOS is a very successful two-parameter equation of state to estimate thermodynamic properties of pure compounds as well as mixtures. The PR EOS has been modified and revised several ways to improve estimates, and the most popular modification is for the attractive term through alpha function and temperature dependent covolume parameter in the repulsive term. However, the unphysical, i.e., negative values of temperature dependent co volume parameter at high temperature lead to undesirable results. We have addressed this issue in the present work by incorporating a temperature dependent covolume parameter and yet physically consistent over a large range of temperature. In the present work, the Modified-Peng-Robinson 2 (MPR2) equation of state is presented by modifying the alpha function in attractive term and temperature dependent co-volume parameter in repulsive term of the PR EOS. The accuracy of MPR2 EOS is demonstrated by comparing results with the PR, HKM1, and MPR1 equations of state. The thermodynamic properties, namely saturated vapor pressure and liquid density, enthalpy of vaporization, compressed liquid densities in sub and supercritical region, heat capacities (isobaric and isochoric), and sound velocity of pure compounds, are predicted by MPR2 EOS which agrees very well with the experimental data. We have further studied 24 refrigerant properties like vapor and liquid densities. The work has also been extended to study the phase behavior of 26 binary mixtures using van der Waals single fluid mixing rules.

Keywords: Alpha Function, Binary Mixture, Co-volume Parameter, Cubic Equation of State, Peng-Robinson, Refrigerants, Thermodynamic Properties

INTRODUCTION

The cubic equation of state (CEOS) plays a vital role in the prediction of PVT properties and phase equilibria in the petroleum industry, reservoir fluids, chemical process design, for example [1]. The reasons for widespread use of CEOS by chemical engineers are [2]: 1) CEOS can be easily extended from pure fluids to mixture;. 2) CEOS can represent almost all fluids. The journey of cubic equations of state started from the van der Waals CEOS. The next breakthrough was Soave's modification of Redlich-Kwong EOS which is popularly known as SRK EOS [3]. The Peng-Robinson EOS was another milestone which could improve limitations of SRK EOS, i.e., vapor pressure and saturated liquid density predictions have been more accurate [4]. The predicted critical compressibility is similar for all two-parameter cubic EOSs that result in saturated liquid density predictions, significantly deviating from the experimental value. Patel-Teja later introduced three parameter CEOS which result in substance dependent critical compressibility factor [5]. This flexibility incorporated by Patel-Teja EOS leads to improved estimation of polar fluid saturated properties. The work has been reported on four and five parameter CEOS in the literature [6-9]. Although Soave-Redlich-Kwong (SRK), Peng-Robinson (PR) and Patel-Teja (PT) are most successful and popular CEOSs used in process engineering calculations, most cubic equations of state predict liquid density with very poor accuracy and accurate prediction of liquid density is very important in the chemical industry [10]. To overcome this problem, two major methodologies have been tried: volume-translated cubic equations of state [11-17] and the temperature dependent co-volume parameter [18-23].

Lopez-Echeverry et al. have written a comprehensive review article on PR EOS and discussed that it has been modified for more than 220 ways either by adjusting its parameters or by extending it to various mixtures [24]. Furthermore, several researchers have studied PR EOS in depth and confirmed that it is clearly a superior cubic equation of state when compared with other contemporary equations of state [25-31]. The PR EOS is a very highly demanded EOS in the petrochemical industry, hence studied and modified extensively to enhance its ability of accurate prediction. There are literally unlimited applications of the PR EOS, including PH prediction [32], energetic materials [33-37], modeling phase behavior of clathrate hydrates [38-44], phase study of monomers and polymers in supercritical fluids [45-54] and various software packages [55]. The better representation of attractive term in the PR equation by introducing the term b(v−b) leads to enhanced liquid density predictions [56]. The PR EOS have been modified in following four major ways by modifying temperature dependent α function in an attractive term of the EOS [57-61], incorporating volume translation [62-66], modifying existing parameters or introducing new parameters in the EOS

†To whom correspondence should be addressed.
E-mail: hsbyun@jnu.ac.kr

[67-69], and introducing modified mixing rules for applications in mixtures [70-75].

Even though PR EOS is explored widely by research and industrial communities, a widely accurate EOS is still needed, which necessitates the continued development and modification in the field [76]. As we mentioned earlier, for pure component applications more than approximately 200 modifications to PR EOS have already been presented in the literature to overcome the limitations of the original PR CEOS. Numerous research articles are published for mixture applications. Nevertheless, these proposed modifications are restricted to systems and properties considered, i.e., PR EOS must be modified and tuned in order to apply for new processes/components/mixtures, which we think is a major drive for consistent proposed modifications in the PR EOS. In present work, we have proposed two modifications, i.e., in both attractive and repulsive parts of the PR EOS. We modified the temperature dependent alpha function in the attractive term and introduced a temperature dependent co-volume term in the repulsive part of the PR EOS. These said modifications have already been incorporated by several authors, e.g., MPR1 (Modified-Peng-Robinson 1) EOS considered in present study for comparison. However, we have observed that for several pure compounds (e.g., methane, ethane, propane, cyclopropane, ethylene, propylene, nitrogen, carbon monoxide etc.), the temperature dependent covolume function proposed in MPR1 EOS turns to unphysical negative values at high temperatures.

The Modified-Peng-Robinson 2 (MPR2) EOS offered in this work with modified alpha function and physically consistent covolume parameter is used to forecast various thermophysical properties of pure fluids like saturated liquid density and vapor pressure, enthalpy of vaporization, compressed liquid densities in sub and supercritical region, velocity of sound, heat capacity (isobaric and isochoric). We compared the results with PR, HKM1 (Haghtalab-Kamali-Mazloumi-Mahmoodi 1) [77] and MPR1 [18] equations of state. All the properties were estimated with acceptable accuracy. The percentage mean average absolute deviation MAAD% of saturated vapor pressure and liquid density over 50 pure compounds using PR, HKM1, MPR1 and MPR2 equations of state is reported. It is 8.94%, 6.79%, 7.04%, and 6.72% for saturated vapor pressure and 7.43%, 7.42%, 5.28%, and 5.20% for saturated liquid density by using PR, HKM1, MPR1, and MPR2 equations of state, respectively. The vapor and liquid density of 24 refrigerants have been further predicted. HKM1, MPR1 and MPR2 EOSs are performing with better accuracy when compared with original PR EOS. The MAAD% in vapor density is 2.68%, 2.16%, 2.54%, and 2.52% for PR, HKM1, MPR1, and MPR2 EOSs, whereas it is 5.62%, 5.27%, 5.33%, and 5.33% for liquid density. The 26 binary mixtures including hydrocarbons as well as monomers in supercritical carbon dioxide were studied using van der Waals one fluid mixing rules. The MAAD% in estimated bubble point pressure is 3.43%, 1.87%, 1.94%, and 2.09% using PR, HKM1, MPR1, and MPR2 EOSs, respectively.

THEORY

1. The Peng-Robinson (PR) Equation of State

The PR EOS [4] is presented as:

$$P = \frac{RT}{v-b} - \frac{a(T)}{v(v+b)+b(v-b)} \tag{1}$$

where,

$$a(T) = 0.457535\frac{\alpha(T)R^2T_c^2}{P_c^2} \tag{2}$$

$$b = 0.077796\frac{RT_c}{P_c} \tag{3}$$

$$\alpha(T) = (1+\kappa(1-\sqrt{T_r}))^2 \tag{4}$$

$$\kappa = 0.37464 + 1.5422\omega - 0.26992\omega^2 \tag{5}$$

where v is the molar volume, P is the pressure, T is the temperature, a and b are EOS parameters, T_c is the critical temperature, P_c is the critical pressure, Z_c is the critical compressibility factor and ω is the acentric factor.

2. Haghtalab-Kamali-Mazloumi-Mahmoodi (HKM1) Equation of State

A three parameter HKM1 EOS [77] is illustrated below:

$$P = \frac{RT}{v-b} - \frac{\alpha(T)}{(v+nb)(v+mc)} \tag{6}$$

$$n = m = -0.5$$

$$Z_c = 0.3181 - 0.0375\omega - 0.0300\omega^2 \tag{7}$$

$$\alpha(T) = \exp[(m_1+m_2T_r)(1-m_3^{lnT_r})] \tag{8}$$

The parameters in Eq. (8) are given below:

$$m_1 = 4.5298 \tag{9}$$

$$m_2 = 2.8698 \tag{10}$$

$$m_3 = 1.0529 + 0.2065\omega - 0.0487\omega^2 \tag{11}$$

3. Modified-Peng-Robinson 1 (MPR 1) Equation of State

The MPR1 EOS [18] is given by modifying alpha function and covolume parameter of attractive and repulsive parts, respectively, of the PR equation of state.

$\alpha(T)$ and b(T) are as given below:

$$\alpha(T) = \exp[(1-m_1^{logT_r})] \tag{12}$$

$$b(T) = 0.07780[1+m_2(1-T_r)] \tag{13}$$

The parameters in Eq. (12) and (13) are given below:

$$m_1 = 0.1554\omega^2 + 1.6571\omega + 1.7309 \tag{14}$$

$$m_2 = 0.1900\omega^2 - 0.8857\omega + 0.2476 \tag{15}$$

4. Modified-Peng-Robinson 2 (MPR 2) Equation of State

The MPR2 EOS proposed modification to the alpha function and co-volume parameter of attractive and repulsive parts respectively of the PR equation of state.

$\alpha(T)$ and b(T) are correlated as given below:

$$\alpha(T) = \exp[m_1(1-T_r)(1+T_r^{m_2})] \tag{16}$$

$$b(T) = \frac{RT_c}{P_c}\beta(T) \tag{17}$$

where, $\beta(T)=\left[m_3\left(1-\frac{1}{T_r^2}\right)+m_4\left(1-\frac{1}{T_r}\right)+m_5\right]$

The generalized form of the parameters in Eq. (16) and (17) are given below:

$$m_1=0.1465\omega^2+0.2525\omega+0.3514 \quad (18)$$

$$m_2=-0.3965\omega^2+1.1064\omega-0.1036 \quad (19)$$

$$m_3=0.0106\omega^2-0.0276\omega+0.0124 \quad (20)$$

$$m_4=-0.0709\omega^2+0.1471\omega-0.0512 \quad (21)$$

$$m_5=-0.0012\omega+0.0783 \quad (22)$$

The parameters m_1, m_2, m_3, m_4 and m_5 are obtained by minimizing of objective function (OF) over reduced temperature range 0.5 to 0.99 using least square fitting technique in Python.

$$OF=\sum_{T_r=0.5}^{0.99} 0.8\frac{|P_{cal}-P_{exp}|}{P_{exp}}+0.2\frac{|\rho_{cal}-\rho_{exp}|}{\rho_{exp}} \quad (23)$$

Here subscripts 'cal' and 'exp' denote theoretical and experimental

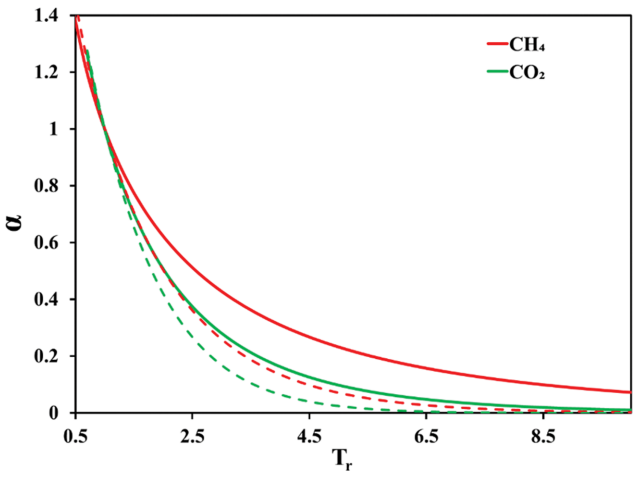

Fig. 1. Plot of the alpha function vs temperature for MPR1 (straight line) and MPR2 (broken line) equations of state.

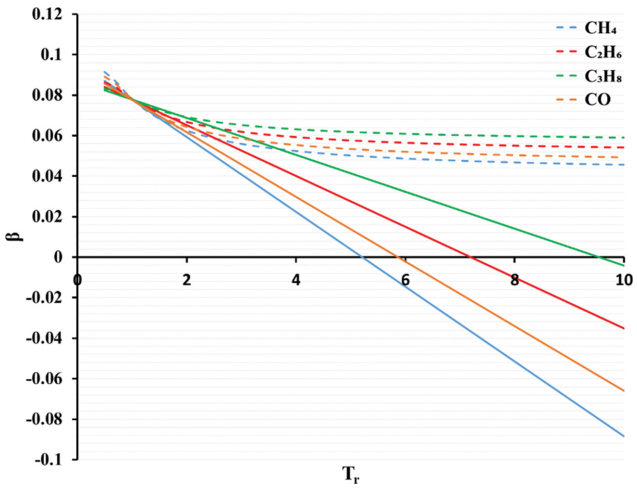

Fig. 2. Beta function (co-volume parameter) variation with temperature using MPR1 (solid lines) and MPR2 (broken lines) EOSs.

Table 1. The pure components along with properties: critical pressure, critical temperature, and acentric factor. The experimental data is taken from Ref. [78]

No	Components	T_r range	P_c (MPa)	T_c (K)	ω
1	Methane	0.5-0.99	4.599	190.564	0.0115
2	Ethane	0.5-0.99	4.872	305.32	0.0995
3	Propane	0.5-0.99	4.248	369.83	0.1523
4	Butane	0.5-0.99	3.796	425.12	0.2002
5	Pentane	0.5-0.99	3.37	469.7	0.2515
6	Hexane	0.5-0.99	3.025	507.6	0.3013
7	Heptane	0.5-0.99	2.74	540.2	0.3495
8	Octane	0.5-0.99	2.49	568.7	0.3996
9	Nonane	0.5-0.99	2.29	594.6	0.4435
10	Decane	0.5-0.99	2.11	617.7	0.4923
11	Pentadecane	0.5-0.99	1.48	708	0.6863
12	Hexadecane	0.5-0.99	1.4	723	0.7174
13	Heptadecane	0.5-0.99	1.34	736	0.7697
14	Octadecane	0.5-0.99	1.27	747	0.8114
15	Nonadecane	0.5-0.99	1.21	758	0.8522
16	Eicosane	0.5-0.99	1.16	768	0.9069
17	Cyclopropane	0.5-0.99	5.54	398	0.1278
18	Cyclohexane	0.5-0.99	4.08	553.8	0.2081
19	2-Methylbutane	0.5-0.99	3.38	460.4	0.2279
20	2-Methylpentane	0.5-0.99	3.04	497.7	0.2791
21	1,3,5-Trinitrobenzene	0.5-0.99	3.39	846	0.8623
22	Nitrogen	0.5-0.99	3.4	126.2	0.0377
23	Oxygen	0.5-0.99	5.04	154.58	0.0222
24	Fluorine	0.5-0.99	5.17	144.12	0.053
25	Carbon monoxide	0.5-0.99	3.5	132.92	0.0482
26	Carbon dioxide*	0.7-0.99	7.38	304.21	0.2236
27	Neon	0.5-0.99	26.5	44.4	–0.0396
28	Argon	0.5-0.99	48.9	150.86	0.0
29	Nitrogen trifluoride	0.5-0.99	44.6	234	0.12
30	Sulfur dioxide	0.5-0.99	78.8	430.75	0.2454
31	Hydrogen sulfide	0.5-0.99	89.6	373.53	0.0942
32	Methanol	0.5-0.99	8.08	512.5	0.5658
33	Ethanol	0.5-0.99	6.14	514	0.6436
34	1-Propanol	0.5-0.99	5.17	536.8	0.6209
35	2-Propanol	0.5-0.99	4.77	508.3	0.6544
36	1-Butanol	0.5-0.99	4.41	563.1	0.5883
37	2-Butanol	0.5-0.99	4.19	535.9	0.5692
38	1-Pentanol	0.5-0.99	3.90	588.1	0.5748
39	2-Pentanol	0.5-0.99	3.70	561	0.5549
40	Cyclohexanol	0.5-0.99	4.26	650.1	0.369
41	1-Hexanol	0.5-0.99	3.45	611.3	0.5586
42	2-Hexanol	0.5-0.99	3.31	585.3	0.5574
43	1-Heptanol	0.5-0.99	3.09	632.3	0.5621
44	2-Heptanol	0.5-0.99	3.00	608.3	0.5628
45	1-Octanol	0.5-0.99	2.78	652.3	0.5697
46	2-Octanol	0.5-0.99	2.75	629.8	0.5807
47	1-Nonanol	0.5-0.99	2.53	670.9	0.5841
48	2-Nonanol	0.5-0.99	2.54	649.5	0.5911
49	1-Decanol	0.5-0.99	2.31	688	0.607
50	1-Undecanol	0.5-0.99	2.12	703.9	0.6236

Table 2. AAD% in the vapor pressure and liquid density predicted using various EOSs. The experimental data is obtained from Ref. [78]

No	Components	AAD%							
		Vapor pressure				Liquid density			
		PR	HKM1	MPR1	MPR2	PR	HKM1	MPR1	MPR2
1	Methane	0.67	0.40	0.88	0.82	9.10	3.05	3.19	4.43
2	Ethane	0.59	0.32	0.47	1.32	6.76	2.56	2.99	3.54
3	Propane	0.89	0.59	0.65	1.82	5.62	2.57	3.02	3.17
4	Butane	0.66	0.42	0.61	1.38	4.86	2.62	3.28	3.10
5	Pentane	0.71	0.38	0.67	1.07	3.88	2.75	3.31	3.62
6	Hexane	1.18	0.84	1.19	0.75	3.26	2.82	3.44	4.06
7	Heptane	1.23	0.52	0.90	0.84	3.85	2.84	3.55	4.29
8	Octane	1.20	0.34	0.82	0.72	5.40	2.89	3.66	4.35
9	Nonane	1.56	0.42	0.77	1.03	6.35	3.34	3.82	3.98
10	Decane	2.01	0.33	0.92	1.57	7.39	4.15	4.05	4.06
11	Pentadecane	5.50	1.26	1.05	1.11	13.48	7.75	6.63	5.73
12	Hexadecane	6.88	1.74	1.63	1.37	14.28	8.78	6.95	6.16
13	Heptadecane	7.24	0.59	1.22	1.01	13.97	12.60	5.91	5.46
14	Octadecane	8.60	0.61	1.70	2.03	14.66	14.99	6.09	5.83
15	Nonadecane	10.31	0.38	2.24	4.00	15.18	17.79	6.22	6.24
16	Eicosane	11.05	2.50	4.59	6.06	14.73	23.47	6.21	5.75
17	Cyclopropane	1.23	0.83	0.83	1.99	5.81	3.16	2.90	4.16
18	Cyclohexane	1.75	1.32	1.44	2.57	5.02	2.74	3.55	3.38
19	2-Methylbutane	0.62	0.42	0.60	1.20	4.90	2.98	3.82	3.79
20	2-Methylpentane	1.01	0.45	0.78	1.20	4.08	3.08	3.91	4.14
21	1,3,5-Trinitrobenzene	18.99	21.74	23.86	19.06	16.55	16.94	7.08	7.70
22	Nitrogen	0.91	0.36	0.31	1.10	9.57	3.12	3.97	2.96
23	Oxygen	0.82	0.27	0.41	1.01	9.13	2.86	3.33	3.50
24	Fluorine	0.66	0.24	0.39	1.09	8.76	3.01	3.69	3.05
25	Carbon monoxide	1.41	1.05	0.72	1.94	9.37	3.04	4.00	2.69
26	Carbon dioxide	0.71	0.95	0.86	1.02	4.16	3.39	3.63	3.52
27	Neon	0.69	0.63	1.26	1.96	13.53	5.04	5.61	2.97
28	Argon	0.44	0.61	1.01	1.32	10.32	3.10	3.74	3.21
29	Nitrogen trifluoride	1.81	1.55	1.39	2.74	5.81	3.34	2.81	4.41
30	Sulfur dioxide	3.75	3.29	3.37	4.40	2.88	3.95	3.26	4.53
31	Hydrogen sulfide	1.64	1.39	1.16	2.50	6.66	2.40	2.76	3.55
32	Methanol	4.52	5.91	6.29	6.90	18.12	7.33	13.57	12.30
33	Ethanol	1.77	3.28	2.93	4.93	10.27	9.99	7.40	6.87
34	1-Propanol	8.44	5.45	4.93	4.18	5.72	12.44	7.90	7.43
35	2-Propanol	10.26	6.58	5.92	5.39	6.97	12.94	7.38	6.77
36	1-Butanol	14.76	11.63	11.32	9.96	3.96	11.98	7.68	7.37
37	2-Butanol	19.20	16.04	15.86	14.19	5.03	9.78	6.40	6.04
38	1-Pentanol	13.39	10.39	10.19	8.73	3.55	11.80	7.77	7.55
39	2-Pentanol	23.81	20.22	20.55	17.98	3.09	10.80	6.78	6.49
40	Cyclohexanol	23.64	22.06	22.48	22.08	5.09	2.99	3.87	4.63
41	1-Hexanol	20.30	16.97	16.91	14.98	4.47	10.02	7.06	6.85
42	2-Hexanol	20.28	16.97	17.23	14.96	3.44	10.47	6.86	6.69
43	1-Heptanol	24.19	20.42	20.54	18.12	2.85	12.71	7.39	7.17
44	2-Heptanol	20.15	16.87	16.75	14.93	3.28	10.78	6.86	6.79
45	1-Octanol	22.55	18.86	18.80	16.73	4.54	9.78	5.82	5.62
46	2-Octanol	28.59	24.35	25.00	21.98	6.26	9.57	7.06	7.15
47	1-Nonanol	23.50	19.27	19.48	16.91	7.33	8.30	5.72	5.59
48	2-Nonanol	28.40	24.71	24.53	22.83	2.62	14.06	7.74	7.78
49	1-Decanol	21.25	16.82	16.93	14.62	7.24	9.27	5.50	5.28
50	1-Undecanol	21.35	15.99	16.62	13.69	8.16	8.99	4.64	4.36
	MAAD%	8.94	6.79	7.04	6.72	7.43	7.42	5.28	5.20

quantities, respectively. The experimental inputs, namely critical pressure, critical temperature, and acentric factor, are taken from a standard reference book [78].

RESULTS AND DISCUSSION

1. Application to Pure Fluids and Refrigerants

The proposed modifications in temperature dependent alpha function and covolume parameter are discussed in the above section. The charts of variation of both alpha function and covolume parameter with temperature are given in Fig. 1 and Fig. 2, respectively. As suggested by kinetic theory of gases [79,80], the covolume parameter is needed to be a temperature dependent function. Hence in present work, we have incorporated a temperature dependent covolume parameter. However, in order to overcome thermodynamic inconsistency at high temperature and pressure, the co-volume parameter is formulated such that its temperature dependence becomes negligible with the rise of temperature. Fig. 2, i.e., covolume vs temperature plot for methane, ethane, propane, and carbon dioxide using MPR1 and MPR2 EOSs, clearly illustrates that the covolume parameter proposed in MPR1 EOS leads to unphysical values as temperature rises, whereas in case of MPR2 EOS covolume parameter is almost independent of temperature at extreme conditions. To test the present model, i.e., MPR2 EOS, several pure component thermodynamic properties like saturated vapor pressure, saturated liquid density, heat capacity (isobaric and isochoric), sound velocity, enthalpy of vaporization, and compressed liquid density in sub and supercritical phases were calculated and compared with the experimental results from the literature. We used experimental data from Perry's Chemical Engineers' Handbook [78] and NIST (National Institute of Standards and Technology) [81]. The pure component experimental input properties, namely critical pressure, critical temperature, and acentric factor, are obtained from Perry's Chemical Engineers' Handbook [78] and given in Table 1 for 50 compounds considered in the present study. The results obtained from MPR2 EOS were compared with two parameter Peng-Robinson EOS [82], modified Peng-Robinson (MPR1) EOS [18], and three parameter Haghtalab-Kamali-Mazloumi-Mahmoodi (HKM1) EOS [77].

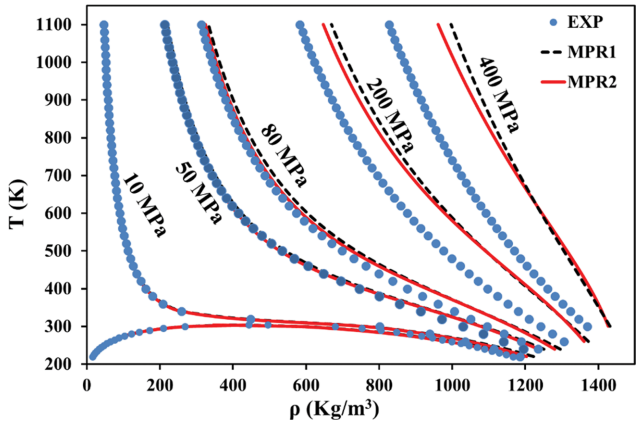

Fig. 3. Experimental and estimated PVT diagram for pure carbon dioxide. The experimental inputs are obtained from NIST [81].

The MAAD% (percentage mean of average absolute deviation) for saturated vapor pressure and liquid density for 50 pure fluids is given in Table 2. The MAAD% is defined as $MAAD\% = \frac{100}{N}\sum_{i=1}^{N}\frac{\left|y_i^{cal} - y_i^{exp}\right|}{y_i^{exp}}$ where, y: given thermodynamic properties under consideration; N: total number of data points. It can be seen that MAAD% in vapor pressure using PR, HKM1, MPR1, and MPR2 EOSs is 8.94%, 6.79%, 7.04%, and 6.72%, while it is 7.43%, 7.42%, 5.28%, and 5.20% for saturated liquid density. It can be very clearly seen that MPR2 EOS is more accurate when compared with PR, MPR1, and HKM1 equations of state for both saturated liquid density and saturated vapor pressure predictions. The PVT behavior of pure carbon dioxide and nitrogen is illustrated in Fig. 3 and Fig. 4, respectively. An expected fit to phase envelopes is observed. It is required to note that both MPR1 and MPR2 EOSs incorporate temperature dependent covolume parameter; however, the liquid density predictions using MPR1 EOS decrease sharply to negative

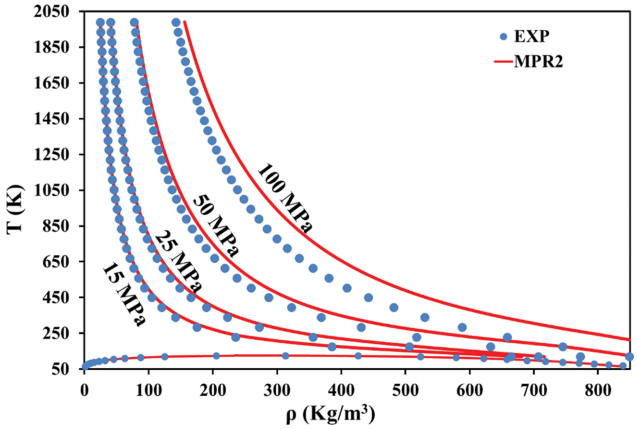

Fig. 4. Experimental and estimated PVT diagram for pure Nitrogen. Unphysical results are obtained using MPR1 EOS. The experimental inputs are obtained from NIST [81].

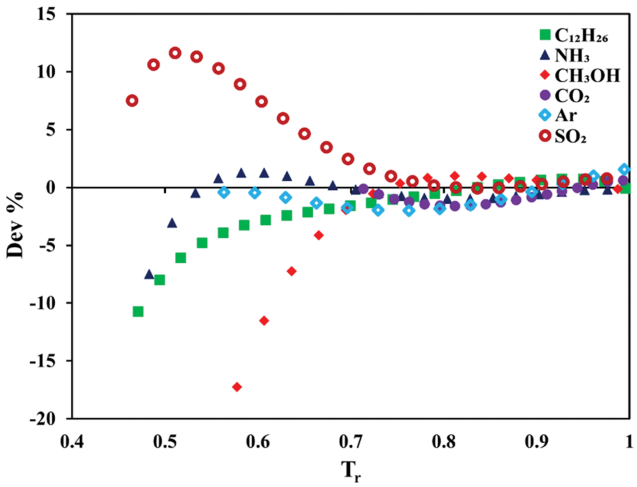

Fig. 5. The variation of percentage deviation of saturated vapor pressure with temperature for various fluids calculated using MPR2 EOS. The experimental inputs are obtained from NIST [81].

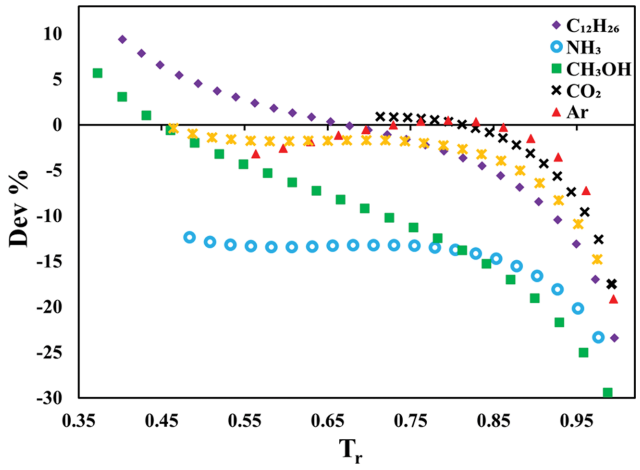

Fig. 6. The variation of percentage deviation in saturated liquid density with temperature for various fluids calculated using MPR2 EOS. The experimental inputs are taken from NIST [81].

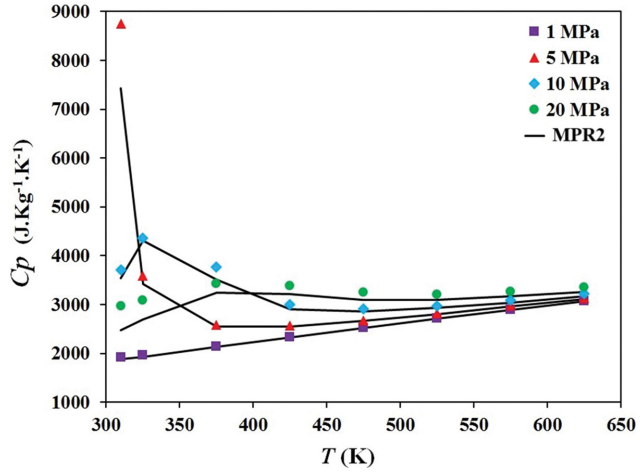

Fig. 7. The predicted and experimental heat capacity of pure ethane at constant pressure. The experimental inputs are obtained from NIST [81].

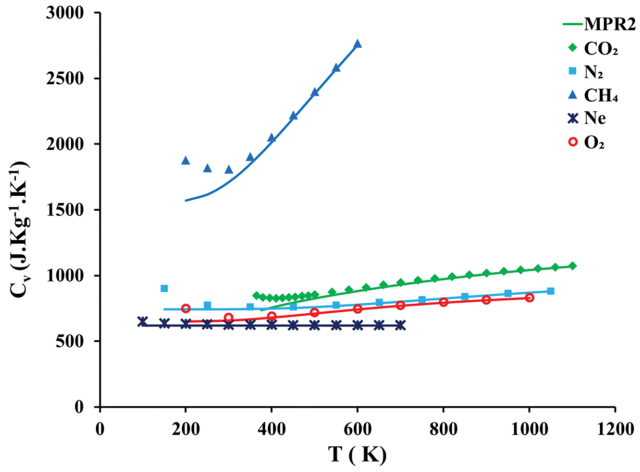

Fig. 8. The predicted and experimental heat capacity at constant volume at 10 MPa pressure for different fluids. The experimental inputs are obtained from NIST [81].

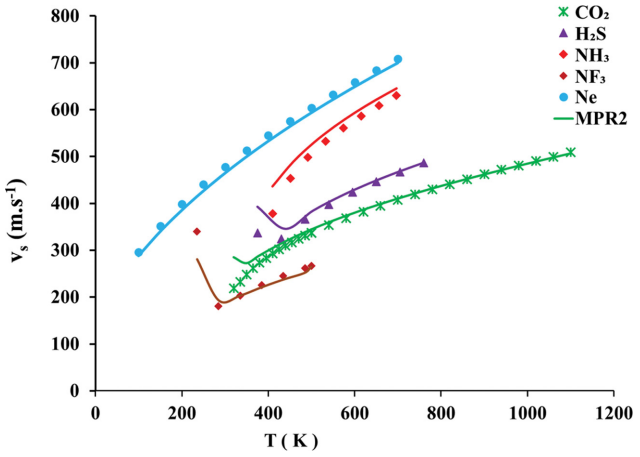

Fig. 9. The predicted and experimental velocity of sound at 10 MPa pressure for various components. The experimental inputs are obtained from NIST [81].

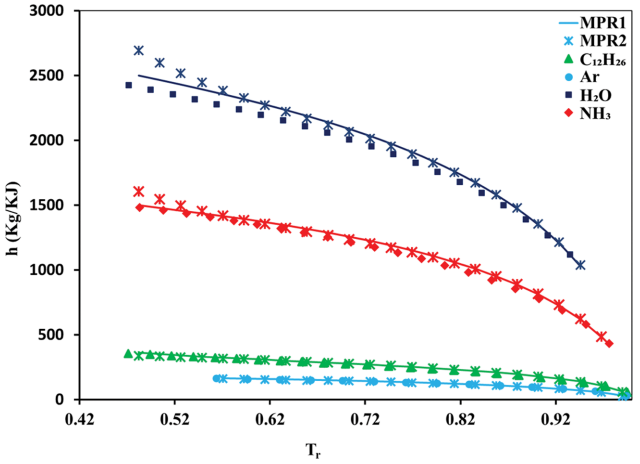

Fig. 10. The predicted and experimental enthalpy of vaporization. The experimental inputs are obtained from NIST [81].

values at high pressure, which gives unphysical results. Hence only predictions of MPR2 EOS are given in Fig. 4.

The percentage deviation, i.e., $100\left(\frac{y_i^{cal}-y_i^{exp}}{y_i^{exp}}\right)$ in vapor pressure and liquid density for different fluids like dodecane, ammonia, methanol, carbon dioxide, sulfur dioxide, and argon against temperature, is given in Fig. 5 and Fig. 6, respectively. The isobaric heat capacity of pure ethane in vapor and supercritical regions for pressure ranging from 1 MPa-20 MPa is shown in Fig. 7. The isochoric heat capacity at pressure of 10 MPa for different fluids like carbon dioxide, nitrogen, methane, neon, and oxygen within a temperature span of 100 K-1,100 K is given in Fig. 8. MPR2 EOS is showing good fit to the experimental data of both isobaric and isochoric heat capacity as illustrated in Fig. 7 and Fig. 8, respectively. The calculated and predicted sound velocity vs temperature plot at 10 MPa pressure for pure components like carbon dioxide, ammonia, hydrogen sulfide, neon and nitrogen trifluoride within a temperature range of 100 K-1,100 K is demonstrated in Fig. 9. Fig. 10 illustrates enthalpy

of vaporization both experimental and predicted using MPR2 EOS for pure fluids including dodecane, argon, water, and ammonia. The predicted results using MPR2 EOS match well with experimental data. The compressed liquid density in subcritical and supercritical regions for methane and ethane are illustrated in Fig. 11 and Fig. 12, respectively. The liquid densities were estimated using MPR1 and MPR2 equations of state for pressures of 10 MPa, 50 MPa, and 100 MPa. As illustrated in Fig. 11 and 12, MPR2 EOS shows the predictions with improved accuracy compared with MPR1

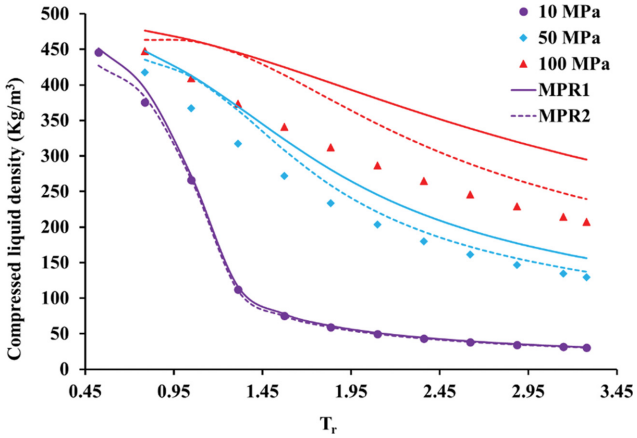

Fig. 11. The predicted and experimental compressed liquid density in sub and supercritical regions for methane. The experimental inputs are obtained from NIST [81].

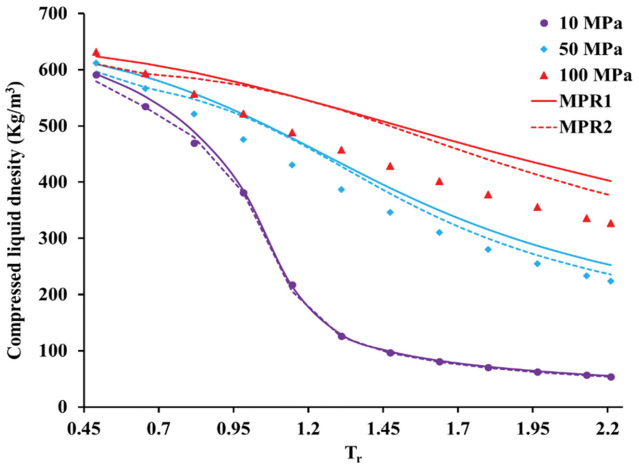

Fig. 12. The predicted and experimental compressed liquid density in sub and supercritical regions for ethane. The experimental data are taken from NIST [81].

Table 3. AAD% predicted using various EOSs of the vapor density and liquid density of various refrigerants. The experimental data is obtained from Ref. [81]

No	Component	AAD%										
		$T_{r\,min}$	$T_{r\,max}$	N	Vapor density				Liquid density			
					PR	HKM1	MPR1	MPR2	PR	HKM1	MPR1	MPR2
1	R11	0.46	1.00	62	1.83	1.16	1.56	2.22	5.63	2.54	3.34	2.33
2	R12	0.45	1.00	54	1.95	1.25	1.69	2.28	5.84	2.64	3.37	2.28
3	R13	0.45	0.97	53	2.55	1.71	2.21	2.86	6.24	2.65	3.50	2.63
4	R14	0.46	0.99	26	1.83	0.92	1.50	2.70	8.05	4.19	5.30	4.27
5	R21	0.45	1.00	51	3.03	2.25	2.67	3.14	4.18	3.02	2.70	2.57
6	R22	0.46	0.99	51	1.75	1.18	1.55	1.99	3.31	3.66	2.69	3.51
7	R23	0.46	1.00	37	1.93	2.60	2.21	2.01	6.36	7.77	7.12	7.65
8	R32	0.46	0.99	43	3.65	4.64	4.24	4.03	14.16	15.03	14.59	14.91
9	R41	0.55	1.00	72	4.75	524	4.99	3.58	13.36	16.21	15.03	16.22
10	R113	0.49	1.00	126	2.08	1.55	1.88	2.54	4.68	3.11	3.86	3.45
11	R114	0.66	1.00	73	6.81	6.62	6.71	7.14	5.00	3.97	4.51	4.10
12	R115	0.49	0.99	89	0.94	0.75	0.96	1.30	4.79	3.10	3.90	3.45
13	R116	0.59	1.00	60	1.24	1.35	1.53	1.63	6.33	4.97	5.68	5.03
14	R123	0.45	1.00	146	2.69	1.73	2.41	2.07	3.40	2.64	3.14	3.42
15	R134a	0.45	1.00	103	2.16	1.14	1.92	1.67	4.48	3.60	3.69	3.89
16	R141b	0.45	1.00	154	2.96	2.13	2.66	3.01	3.99	2.83	2.76	2.77
17	R142b	0.45	1.00	134	2.05	1.30	1.82	2.02	3.25	3.98	3.02	3.79
18	R218	0.45	1.00	110	2.41	1.32	2.11	1.53	5.83	5.90	6.26	6.54
19	R227ea	0.45	1.00	115	2.61	1.36	2.23	1.29	5.18	6.50	6.41	6.90
20	R236ea	0.59	1.00	86	3.00	3.59	3.51	3.17	5.94	7.94	7.24	7.08
21	R236fa	0.45	1.00	110	3.74	1.95	3.12	2.07	2.89	4.39	4.35	5.03
22	R245ca	0.45	0.99	123	3.32	2.12	3.15	2.81	3.34	4.47	4.51	5.04
23	R245fa	0.47	1.00	114	3.60	2.52	3.03	2.13	3.21	4.46	4.53	5.07
24	Rc318	0.60	1.00	78	1.36	1.45	1.33	2.22	5.54	6.81	6.44	6.06
	MAAD%				2.68	2.16	2.54	2.52	5.62	5.27	5.33	5.33

Table 4. The interaction parameter k_{ij} and η_{ij} of binary mixtures using various equations of state

No	Binary mixtures	k_{ij}				η_{ij}			
		PR	HKM1	MPR1	MPR2	PR	HKM1	MPR1	MPR2
1	Methane-Ethane	0.003125	0.003546	0.016431	0.017691	0.002992	0.002985	0.00815	0.008368
2	Methane-Propane	0.002128	−0.005514	0.015963	−0.014332	−0.009165	−0.010829	−0.009333	−0.02513
3	Methane-Butane	0.005823	0.011275	0.018842	−0.004683	−0.009555	0.00081	−0.005838	−0.012409
4	Ethane-Propane	−0.035189	−0.033011	−0.033311	−0.006245	−0.039605	−0.038651	−0.040122	−0.005073
5	Hexane-Heptane	0.005162	0.006147	0.008106	0.00387	0.002543	0.002398	0.002013	0.002924
6	Heptane-Octane	0.004862	0.005208	0.008615	0.005689	0.002621	0.002595	0.001897	0.002562
7	Propylene-Propane	0.008363	0.009856	0.009641	0.011452	0.001917	0.001453	0.001447	0.000972
8	1-Butene.1-Hexene	0.030655	0.031448	0.029647	0.036702	0.034055	0.035837	0.031701	0.039401
9	Carbon dioxide-Propane	0.112694	0.112168	0.101477	0.10482	−0.028749	−0.02866	−0.045631	−0.04273
10	Nitrogen-Propane	0.014664	0.010344	0.100309	−0.037621	−0.042283	−0.028659	−0.055363	−0.068772
11	Nitrogen-Carbon dioxide	0.008552	−0.028322	0.094112	−0.018935	0.001885	0.009178	−0.024757	0.005401
12	Nonane-Cyclohexane	−0.103246	−0.152322	−0.072103	−0.12342	−0.107536	−0.143155	−0.079816	−0.136949
13	Nonane-Toluene	0.008187	−0.001985	0.013426	0.011655	0.002024	0.004127	0.000408	0.000893
14	Nonane-m-Xylene	0.011577	0.008363	0.01614	0.014032	0.000999	0.001917	−0.000364	0.000257
15	Nonane-p-Xylene	−0.006658	−0.008964	−0.000993	−0.002427	0.005283	0.005839	0.003917	0.004387
16	Heptane-o-Xylene	0.009472	0.006806	0.011606	0.009267	0.001563	−0.002329	0.000893	0.001672
17	Heptane-m-Xylene	0.00593	0.011499	0.008118	0.009551	0.002472	0.007894	0.002087	0.007242
18	Heptane-p-Xylene	−0.013445	−0.011027	−0.007122	−0.008792	−0.019999	−0.018306	−0.015431	−0.014013
19	Heptane-Ethylbenzene	0.002165	0.002718	0.012174	0.01303	0.003361	0.003206	0.011728	0.016484
20	Benzene-Toluene	−0.003657	−0.001594	−0.000391	−0.00762	0.00453	0.004106	0.003788	0.005344
21	Toluene-m-Xylene	0.010747	0.012941	0.013424	0.008827	0.001328	0.000584	0.000497	0.001717
22	Toluene-o-Xylene	−0.000663	0.001609	0.001778	−0.050011	0.003857	0.003365	0.003381	−0.047456
23	Vinyl benzoate-SC Carbon dioxide	0.030234	0.017658	0.021033	0.002354	−0.061645	−0.047172	−0.064802	−0.066807
24	Vinyl pivalate-SC Carbon dioxide	0.010964	0.049914	0.051847	0.035367	0.001291	−0.018472	−0.031312	−0.046019
25	Vinyl octanoate-SC Carbon dioxide	0.01326	0.042417	0.045313	0.02467	0.000397	−0.008183	−0.009317	−0.003029
26	Tridecyl methacrylate-SC Carbon dioxide	0.055396	0.021466	0.036869	0.032492	−0.03157	−0.027726	−0.024746	−0.02237

EOS.

We further considered to predict properties of 24 refrigerants using PR, HKM1, MPR1, and MPR2 EOSs. As shown in Table 3, vapor and liquid volumes for refrigerants have been predicted. The MAAD% in predicted vapor density is 2.68%, 2.16%, 2.54%, and 2.52% using PR, HKM1, MPR1, and MPR2 EOS, respectively, whereas for predicted liquid density it is 5.62%, 5.27%, 5.33%, and 5.33%, respectively. The refrigerants experimental data required are taken from NIST [81]. It is observed that HKM1, MPR1, and MPR2 have been shown to predict refrigerants properties with better accuracy when compared with the predictions of original PR EOS.

The expressions used for calculations of the above-mentioned properties are given in Appendix A.

2. Application to Binary Mixtures

To be able to predict mixture phase behavior is one of the crucial applications of any EOS. Hence, the present work was further extended to various binary mixtures, including hydrocarbons as well as mixtures of monomers in supercritical carbon dioxide. The van der Waals single fluid mixing rules with a couple of interaction parameters were used in the present work.

$$a = \sum_{1}^{n}\sum_{1}^{n} x_i x_j a_{ij}$$

$$b = \sum_{1}^{n}\sum_{1}^{n} x_i x_j b_{ij}$$

Here, n: number of components in the mixture. a_{ij} and b_{ij} are defined as, $a_{ij} = (a_{ii}a_{jj})^{1/2}(1-k_{ij})$ and $b_{ij} = \frac{1}{2}(b_{ii}+b_{jj})(1-\eta_{ij})$ and the parameters k_{ij} and η_{ij} are found by using objective function given

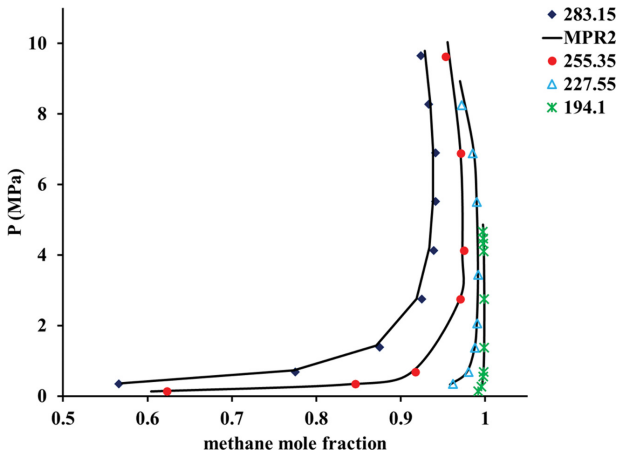

Fig. 13. Phase behavior diagram of CH_4-C_4H_{10} binary mixture.

Table 5. AAD% of the bubble pressure for different binary mixtures is calculated using various equations of state

No	Binary mixtures	AAD% in bubble pressure					Ref
		N	PR	HKM1	MPR1	MPR2	
1	Methane-Ethane	116	1.61	1.71	1.42	1.47	[83]
2	Methane-Propane	123	1.53	1.77	1.81	2.84	[83]
3	Methane-Butane	72	3.14	3.66	3.30	3.03	[84]
4	Ethane-Propane	83	1.32	1.33	1.35	1.01	[85]
5	Hexane-Heptane	22	0.48	0.44	0.42	0.53	[86]
6	Heptane-Octane	6	0.84	0.72	0.75	0.84	[86]
7	Propylene-Propane	84	0.22	0.21	0.25	0.26	[87]
8	1-Butene-1-Hexene	4	0.55	0.59	0.57	0.63	[88]
9	Carbon dioxide-Propane	52	0.69	0.70	0.67	0.61	[89]
10	Nitrogen-Propane	29	1.68	1.93	3.36	3.68	[90]
11	Nitrogen-Carbon dioxide	23	3.33	2.43	2.53	2.98	[91]
12	Nonane-Cyclohexane	6	1.49	1.52	1.71	1.31	[92]
13	Nonane-Toluene	14	1.26	1.35	1.57	1.19	[92]
14	Nonane-m-Xylene	13	0.30	0.45	0.50	0.48	[92]
15	Nonane-p-Xylene	12	0.26	0.24	0.26	0.44	[92]
16	Heptane-o-Xylene	20	0.18	0.11	0.18	0.25	[93]
17	Heptane-m-Xylene	21	0.10	0.11	0.28	0.09	[93]
18	Heptane-p-Xylene	21	0.09	0.07	0.20	0.13	[93]
19	Heptane-Ethylbenzene	17	0.10	0.15	0.26	0.15	[93]
20	Benzene-Toluene	8	0.85	0.69	0.78	1.32	[86]
21	Toluene-m-Xylene	22	1.58	1.47	1.55	1.70	[86]
22	Toluene-o-Xylene	22	1.12	1.23	1.26	1.22	[86]
23	Vinyl benzoate-Carbon dioxide	60	27.38	7.96	7.66	7.37	[94]
24	Vinyl pivalate-Carbon dioxide	65	15.35	5.37	5.18	5.84	[94]
25	Vinyl octanoate-Carbon dioxide	66	18.27	5.65	5.84	7.34	[94]
26	Tridecyl methacrylate-Carbon dioxide	13	5.45	6.71	6.82	7.76	[46]
	MAAD%		3.43	1.87	1.94	2.09	

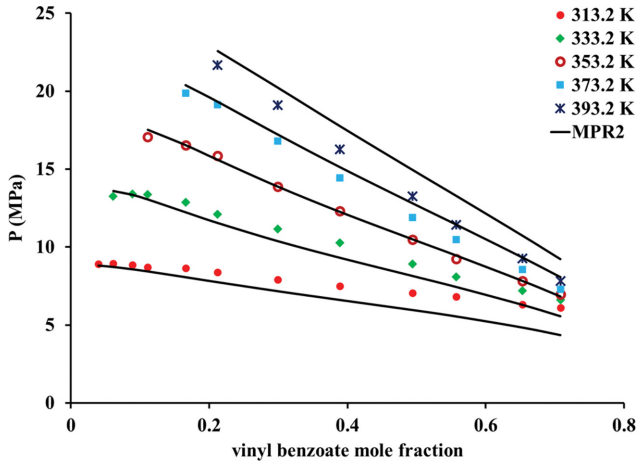

Fig. 14. Phase behavior diagram of a vinyl benzoate-supercritical carbon dioxide binary mixture.

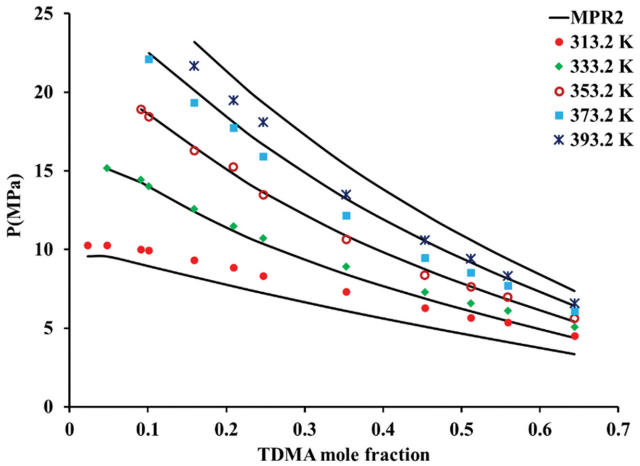

Fig. 15. Phase behavior diagram of a TDMA (tridecyl methacrylate) - supercritical carbon dioxide binary mixture.

below:

$$OF = \sum_{i=1}^{N} \left(\frac{P_i^{exp} - P_i^{cal}}{P_i^{exp}} \right)^2$$

Where P_i^{exp} and P_i^{cal} are experimental and estimated bubble point pressure, respectively. N refers to the total number of experimental pressure data points.

We considered 26 binary mixtures to predict bubble point pres-

sure. The list of corresponding interaction parameters k_{ij} and η_{ij} for PR, HKM1, MPR1, and MPR2 EOSs is given in Table 4. The MAAD% in estimated bubble point pressure is approximately in the range of 1.8-3.4% using PR, HKM1, MPR1, and MPR2 EOSs as given in Table 5. We have demonstrated predicted vapor liquid phase behavior diagram of binary mixtures of CH_4-C_4H_{10}, vinyl benzoate-supercritical carbon dioxide, and TDMA (tridecyl methacrylate) - supercritical carbon dioxide in Figs. 13, 14, and 15, respectively, using MPR2 EOS. These figures clearly show that estimations are in decent agreement with the experimental results with the simple mixing rules.

CONCLUSION

The MPR2 EOS was introduced by incorporating temperature-dependent functions in both attractive and repulsive terms of PR EOS. The results obtained for vapor pressure and liquid density for 50 compounds were estimated with the MPR1, HKM1 and PR equation of state. The estimated MAAD% is 9.01%, 6.85%, 7.10%, and 6.80% for saturated vapor pressure and 7.43%, 7.40%, 5.26%, and 5.19% for saturated liquid density using PR, HKM1, MPR1, and MPR2 equations of state, respectively. The other thermodynamic properties like heat capacity (isobaric and isochoric), compressed liquid density, sound velocity, and enthalpy of vaporization of pure substances were predicted and illustrated graphically. The 24 refrigerants were also studied in the present work. The properties like vapor and liquid densities were predicted. The HKM1, MPR1, and MPR2 EOSs were observed to be performing with better accuracy when compared with original PR EOS predictions.

The MPR2 EOS was extended for the application of binary mixture phase behavior prediction. The simple van der Waals mixing rules with two interaction parameters were used for bubble pressure prediction. The bubble pressure was estimated in the MAAD% range of 1.8-3.4% for PR, HKM1, MPR1, and MPR2 EOSs. Hence, we can conclude that MPR2 EOS is performing with acceptable accuracy when compared with other equations of state.

ACKNOWLEDGEMENT

This work was supported financially by the grant of National Research Foundation of Korea (NRF) financed by the Korea government (MSIT) (No. 2021R1A2C2006888).

DECLARATION OF COMPETING INTEREST

Conflict of interest none declared.

SYMBOLS USED

Symbols

a : attraction parameter [$Pa \cdot m^6 \cdot mol^{-2}$]
b : co-volume parameter [$m^3 \cdot mol^{-1}$]
C_p : isobaric molar heat capacity [$J \cdot mol^{-1} \cdot K^{-1}$]
C_v : isochoric molar heat capacity [$J \cdot mol^{-1} \cdot K^{-1}$]
h : molar enthalpy [$KJ \cdot mol^{-1}$]
N : number of data inputs
P : pressure [Pa]
R : universal gas constant 8.314462 [$J \cdot mol^{-1} \cdot K^{-1}$]
T : temperature [K]
v : molar volume [$m^3 \cdot mol^{-1}$]
v_s : sound velocity [$m \cdot s^{-1}$]

Greek Letters

α : alpha function
β : beta function
ω : pitzer acentric factor

Subscripts

c : critical
G : vapor phase
L : liquid phase
r : reduced

Superscripts

cal : calculated
exp : experimental

REFERENCES

1. H. Li, Cham, Cubic equation of state, In: *Multiphase equilibria of complex reservoir fluids*, Springer, Alberta (2021).
2. J. M. Prausnitz and F. W. Tavares, *AIChE J.*, **50**, 739 (2004).
3. G. Soave, *Chem. Eng. Sci.*, **27**, 1197 (1972).
4. D. Y. Peng and D. B. Robinson, *Ind. Eng. Chem. Fundam.*, **15**, 59 (1976).
5. N. C. Patel and A. S. Teja, *Chem. Eng. Sci.*, **37**, 463 (1982).
6. P. N. P Ghoderao, V. H. Dalvi and M. Narayan, *Chem. Eng. Sci.*, **190**, 173 (2018).
7. P. N. P. Ghoderao, V. H. Dalvi and M. Narayan, *Chin. J. Chem. Eng.*, **27**, 1132 (2019).
8. P. N. P Ghoderao, V. H. Dalvi and M. Narayan, *Chem. Eng. Sci. X.*, **3**, 100026 (2019).
9. N. Kukreja, P. N. P. Ghoderao, V. H. Dalvi and M. Narayan, *Fluid Phase Equilib.*, **531**, 112908 (2021).
10. J. O. Valderrama and M. Alfaro, *Oil. Gas Sci. Technol.*, **55**, 523 (2000).
11. A. Peneloux, R. E. Rauzy and R. Freze, *Fluid Phase Equilib.*, **8**, 7 (1982).
12. P. Watson, M. Casella, S. Salerno and D. Tassios, *Fluid Phase Equilib.*, **27**, 35 (1986).
13. J. C. Tsai and Y. P. Chen, *Fluid Phase Equilib.,* **145**, 193 (1998).
14. H. B. D. Sant'Ana, P. Ungerer and J. C. D. Hemptinne, *Fluid Phase Equilib.*, **154**, 193 (1999).
15. X. Chen and H. Li, *Fluid Phase Equilib.*, **521**, 112724 (2020).
16. K. Frey, M. Modell and J. Tester, *Fluid Phase Equilib.*, **279**, 56 (2006).
17. X. Chen and H. Li, *Fluid Phase Equilib.*, **528**, 112852 (2021).
18. A. Haghtalab, P. Mahmoodi and S. H. Mazloumi, synthetic natural gas, and gas condensate mixtures, *Can. J. Chem. Eng.*, **89**, 1376 (2011).
19. G. G. Fuller, *Ind. Eng. Chem. Fundam.*, **15**, 254 (1976).
20. A. Dashtizadeh, G. R. Pazuki, V. Taghikhani and C. Ghotbi, *Fluid Phase Equilib.*, **242**, 19 (2006).

21. A. H. Farrokh-Niae, H. Moddarress and M. Mohsen-Nia, *J. Chem. Thermodyn.*, **40**, 84 (2008).
22. M. M. Nia, H. Modarress and G. A. Mansoori, *Fluid Phase Equilib.*, **206**, 27 (2003).
23. H. Hinojosa-Gomez, J. F. Barragan-Aroche and E. R. Bazua-Rueda, *Fluid Phase Equilib.*, **298**, 12 (2010).
24. J. S. Lopez-Echeverry, S. Reif-Acherman and E. Araujo-Lopez, *Fluid Phase Equilib.*, **447**, 39 (2017).
25. M. S. Zabaloy and J. H. Vera, *Ind. Eng. Chem. Res.*, **37**, 1591 (1998).
26. M. Ghanbari, M. Ahmadi and A. Lashanizadegan, *Cryogenics*, **84**, 13 (2017).
27. M. R. Faradonbeh, J. Abedi and T. G. Harding, *Can. J. Chem. Eng.*, **91**, 101 (2013).
28. J. O. Valderrama, *Ind. Eng. Chem. Res.*, **42**, 1603 (2003).
29. R. R. Tarakad, C. F. Spencer and S. B. Adler, *Ind. Eng. Chem. Process. Des. Dev.*, **4**, 726 (1979).
30. P. Ghosh, *Chem. Eng. Technol.*, **22**, 379 (1999).
31. G. W. Vera and J. H. Vera, *AIChE J.*, **61**, 2824 (2015).
32. T. Tsuji, M. Shigeru, T. A. Hoshina, K. Yoneda, T. Funazukuri and N. A. Morad, *Fluid Phase Equilib.*, **441**, 9 (2017).
33. M. Chen, Y. Xie, H. Wu, S. Shi and J. Yu, *Appl. Therm. Eng.*, **110**, 47 (2017).
34. M. Mehrpooya, F. Gharagheizi and A. Vatani, *Int. J. Energy Res.*, **33**, 960 (2009).
35. M. Mehrpooya, M. Hossieni and A. Vatani, *Ind. Eng. Chem. Res.*, **53**, 17705 (2014).
36. M. Mehrpooya, A. Vatani and A. Mousavian, *Chem. Eng. Process. Process Intensif.*, **49**, 376 (2010).
37. J. S. Brown, *Int. J. Refrig.*, **30**, 1319 (2007).
38. D. R. Bhawangirkar, J. Adhikari and J. S. Sangwai, *J. Chem. Thermodyn.*, **117**, 180 (2018).
39. J. N. Anil, D. R. Bhawangirkar and J. S. Sangwai, *Fluid Phase Equilib.*, **556**, 113356 (2022).
40. V. R. Avula, R. L. Gardas and J. S. Sangwai, *J. Chem. Thermodyn.*, **85**, 163 (2015).
41. V. R. Avula, R. L. Gardas and J. S. Sangwai, *J. Nat. Gas Sci. Eng.*, **33**, 509 (2016).
42. V. R. Avula, R. L. Gardas and J. S. Sangwai, *Fluid Phase Equilib.*, **382**, 187 (2014).
43. V. R. Avula, P. Gupta, R. L. Gardas and J. S. Sangwai, *Asia-Pac. J. Chem. Eng.*, **12**, 709 (2017).
44. A. Joshi, P. Mekala and J. S. Sangwai, *J. Nat. Gas Chem.*, **21**, 459 (2012).
45. P. N. P. Ghoderao, D. Dhamodharan and H. S. Byun, *J. Chem. Thermodyn.*, **168**, 106746 (2022).
46. P. N. P. Ghoderao, D. Dhamodharan and H. S. Byun, *New J. Chem.*, **46**, 2300 (2022).
47. D. Dhamodharan, P. N. P. Ghoderao, C. W. Park and H. S. Byun, *New J. Chem.*, **46**, 7271 (2022).
48. D. Duraisami, P. W. Cheol, P. N. P. Ghoderao and H. S. Byun, *J. Ind. Eng. Chem.*, **367**, 110 (2022).
49. H. S. Byun, *J. Ind. Eng. Chem.*, **99**, 158 (2021).
50. C. W. Park, C. H. Kim and H. S. Byun, *Korean J. Chem. Eng.*, **38**, 610 (2021).
51. H. S. Byun, *J. Ind. Eng. Chem.*, **90**, 76 (2020).
52. D. Duraisami, P. N. P. Ghoderao and H. S. Byun, *J. Mol. Liq.*, **357**, 119112 (2022).
53. S. H. Choa, B. S. Lee and H. S. Byun, *J. CO_2 Util.*, **25**, 39 (2018).
54. B. S. Lee and H. S. Byun, *J. Supercrit. Fluids*, **135**, 211 (2018).
55. V. Diky, R. D. Chirico, C. D. Munzy, A. F. Kazakov, K. Kroenlein, J. W. Magee, I. Abdulagatov and M. Frenkel, *J. Chem. Inf. Model.*, **53**, 3418 (2013).
56. S. I. Sandler, *Models for thermodynamic and phase equilibria calculations*, Marcel Dekker Inc., New Jersey (1994).
57. A. Kumar and R. Okuno, *Fluid Phase Equilib.*, **335**, 46 (2021).
58. A. Kumar and R. Okuno, *Ind. Eng. Chem. Res.*, **53**, 440 (2014).
59. H. Li, *Phase behaviour and mass transfer of solvent(s)-CO_2-heavy oil systems under reservoir conditions*, Ph.D. thesis, University of Regina (2013).
60. P. Mahmoodi and M. Sedigh, *J. Supercrit. Fluids*, **120**, 191 (2017).
61. R. Privat, M. Visconte, A. Z. Khames and J. N. Jaubert, *Chem. Eng. Sci.*, **126**, 584 (2015).
62. J. Hekayati, A. Roosta and J. Javanmardi, *Korean J. Chem. Eng.*, **33**, 3231 (2016).
63. L. A. Forero and J. A. Velasquez, *Fluid Phase Equilib.*, **418**, 74 (2016).
64. A. K. Singh, J. O. Delfs, N. Bottcher, J. Taron, W. Wang, U. J. Gorke and O. Kolditz, *Energy Procedia*, **37**, 3901 (2013).
65. A. Diedrichs, J. Rarey and J. Gmehling, *Fluid Phase Equilib.*, **248**, 56 (2006).
66. J. Ahlers and J. Gmehling, *Fluid Phase Equilib.*, **191**, 177 (2001).
67. P. C. Myint, M. A. McClellandv and A. L. Nichols, *Ind. Eng. Chem. Res.*, **55**, 2252 (2016).
68. S. Kaviani, F. Feyi and B. Khosravi, *Phy. Chem. Liq.*, **54**, 545 (2015).
69. A. Kumar and R. Okuno, *Chem. Eng. Sci.*, **127**, 293 (2015).
70. S. E. K. Fateen, M. M. Khalil and A. O. Elnabawy, *J. Adv. Res.*, **4**, 137 (2013).
71. A. V. Venkatramani and R. Okuno, *J. Nat. Gas. Sci. Eng.*, **26**, 1091 (2015).
72. X. Li, D. Yang, X. Zhang, G. Zhang and J. Gao, *Fluid Phase Equilib.*, **417**, 77 (2016).
73. A. M. Abudour, S. A. Mohammad and K. A. M. Gasem, *Fluid Phase Equilib.*, **319**, 77 (2012).
74. H. Zhang, M. Gong, H. Li, Y. Zhao, Q. Zhong, X. Dong, J. Shen and J. Wu, *Fluid Phase Equilib.*, **425**, 374 (2016).
75. S. Martynov, S. Brown and H. Mahgereftech, *Greenh. Gases Sci. Technol.*, **3**, 136 (2013).
76. M. Erdogmus and M. A. Adewumi, *A modified equation of state for gas condensate systems*, Society of petroleum engineers, Morgantoen, West Virginia (2000).
77. A. Haghtalab, M. J. Kamali, S. H. Mazloumi and P. Mahmoodi, *Fluid Phase Equilib.*, **293**, 209 (2010).
78. D. W. Green and R. H. Perry, *Perry's chemical engineer's handbook*, 8th ed., McGraw-Hill, New-York (2007).
79. J. O. Valderrama, *J. Supercrit. Fluids*, **55**, 415 (2010).
80. L. B. Loeb, *The kinetic theory of gases*, 3rd ed., Dover publications, New York (2004).
81. P. J. Linstrom, *National institute of standard and technolgy*, Standard Reference Database. (2005). http://webbook.nist.gov/chemistry/fluid/.
82. D. Y. Peng and D. B. Robinson, *Ind. Eng. Chem. Fundam.*, **15**, 59 (1976).
83. I. Wichterle and R. Kobayashi, *J. Chem. Eng. Data*, **17**, 9 (1972).

84. L. C. Kahre, *J. Chem. Eng. Data*, **19**, 67 (1974).
85. C. J. Blanc and J. C. B. Setler, *J. Chem. Eng. Data*, **33**, 111 (1988).
86. K. J. Lee, W. K. Chen, J. W. Ko, L. S. Lee and C. M. J. Cheng, *J. Taiwan Inst. Chem. Eng.*, **40**, 573 (2009).
87. Q. N. Ho, K. S. Yoo, B. G. Lee and J. S. Lim, *Fluid Phase Equilib.*, **245**, 63 (2006).
88. S. Laugier and D. Richon, *J. Chem Eng. Data*, **41**, 282 (1996).
89. J. H. Kim and M. S. Kim, *Fluid Phase Equilib.*, **238**, 13 (2005).
90. B. Yucelen and A. J. Kidnay, *J. Chem Eng. Data*, **44**, 926 (1999).
91. F. A. Somait and A. J. Kidnay, *J. Chem Eng. Data*, **23**, 301 (1978).
92. B. S. Gupta and M. J. Lee, *Fluid Phase Equilib.*, **313**, 190 (2012).
93. C. Diaz and J. Tojo, *J. Chem. Thermodyn.*, **34**, 1975 (2002).
94. P. N. P. Ghoderao, D. Duraisami, S. Mubarak and H. S. Byun, *J. Mol. Liq.*, **358**, 119131 (2022).

APPENDIX A

1. Fugacity coefficient (ϕ) of the pure components using PR:

$$\ln\phi=(Z-1)-\ln\left(Z-\frac{bP}{RT}\right)-\frac{a}{2\sqrt{2}bRT}\ln\left[\frac{Z+(1+\sqrt{2})bP/RT}{Z+(1-\sqrt{2})bP/RT}\right]$$

2. Fugacity coefficient of the pure components using HKM1 EOS:

$$\ln\phi=(Z-1)-\ln\left(Z-\frac{bP}{RT}\right)-\frac{a/RT}{mc-nb}\ln\left[\frac{Z+nbP/RT}{Z+mcP/RT}\right]$$

3. Pure fluid heat capacity (isobaric and isochoric):

$$C_v=C_v^{IG}+T\int_{\infty}^{v}S_3\,dv$$

$$C_p=C_p^{IG}-\underset{\sim}{R}+T\int_{\infty}^{v}S_3\,dv-T\frac{S_1^2}{S_2}$$

IG: Ideal gas state, $S_1=\left(\frac{\delta P}{\delta T}\right)_v$, $S_2=\left(\frac{\delta P}{\delta v}\right)_T$, and $S_3=\left(\frac{\delta^2 P}{\delta T^2}\right)_v$

4. Sound velocity:

$$v_s^2=-\left(\frac{C_p}{C_v}\right)\frac{v^2}{M}\left(\frac{\delta P}{\delta v}\right)_T$$

where M : molecular weight.

5. Enthalpy of vaporization:

$$\Delta h^{vap}(T,P)=RT(Z_G-Z_L)+\int_{v_L}^{v_G}\left[T\left(\frac{\partial P}{\partial T}\right)_v-P\right]dv$$

where G denotes the gaseous phase and L denotes the liquid phase

For derivative and integration, libraries in Python were used.